Intrinsic Noise Characteristics of AlGaN/GaN HEMTs

Sungjae Lee[1], Vinayak Tilak[2], Kevin J. Webb[1], and Lester F. Eastman[2]
[1]School of Electrical and Computer Engineering, Purdue University, West Lafayette, IN 47907
[2]School of Electrical Engineering, Cornell University, Ithaca, NY 14853

Abstract— **Intrinsic noise sources and their correlation in AlGaN/GaN HEMTs are extracted and studied. Using three noise parameters obtained from microwave noise measurements and S-parameter data, two intrinsic noise sources and their correlation are specified by applying a noise deembedding technique, and their dependence on frequency and bias point is investigated.**

I. Introduction

Recently, wide bandgap aluminum gallium nitride/gallium nitride (AlGaN/GaN) high electron mobility transistors (HEMTs) have been extensively studied for high frequency, high power operation due to their high saturated electron drift velocity and large breakdown voltage combined with good thermal conductivity. Although GaN-based HEMTs are currently being considered for high power and high temperature operation in the transmitter system [1], recent research has shown that AlGaN/GaN HEMTs also can have low noise characteristics. Low $1/f$ noise is important in transmitter oscillators. This low frequency noise in AlGaN/GaN HEMTs has been studied recently [2]. Low-noise characteristics, as well as the reduced possibility of receiver damage due to the high breakdown field, presents opportunities for high-performance, robust receiver design in GaN. A minimum microwave noise figure of 0.53 dB at 8 GHz (100 GHz f_T device, V_d = 8 V) and 0.4 dB at 5 GHz (58 GHz f_T device, V_d = 1 V) have been reported [3], [4], indicating promising results compared with GaAs technology.

Complete HEMT noise characterization requires measurements from zero frequency through the microwave range, and then determination of a noise equivalent circuit. This can allow the analysis of oscillator phase noise, receiver noise, and the influence of physical effects such as traps of various speeds. Without determination of this accurate model, the various noise source contributions cannot be determined and hence many device and material approaches to reduce noise cannot be ascertained. Most microwave device noise characterization seeks simply to determine a minimum noise figure. The establishment of a noise model for the AlGaN/GaN HEMT will allow study of microwave noise mechanisms within the device.

As suggested by Rothe and Dahlke [5], all noise within a two-port device can be represented as two equivalent and partially correlated noise sources (a voltage and a current source) at the input of the same two-port device, now considered noiseless, as shown in Fig. 1 (a). Through the definition of a correlation impedance, Z_c, two independent noise sources (v_u, i_A) can be used, as in Fig. 1 (b). This allows the convenient expression of the two-port noise figure and other noise parameters. Measurement of a two-port noise figure for various source admittances allows the determination of three variables, NF_{min} (minimum noise figure), R_N (noise voltage source equivalent resistance), and Y_{opt} (the optimum source admittance) by means of a least mean square error fit, from which the fundamental noise sources at the input of the noiseless two-port can be determined. These types of measurements are common, and much work has been done to relate these results to the various noise sources within the device [6], [7], [8].

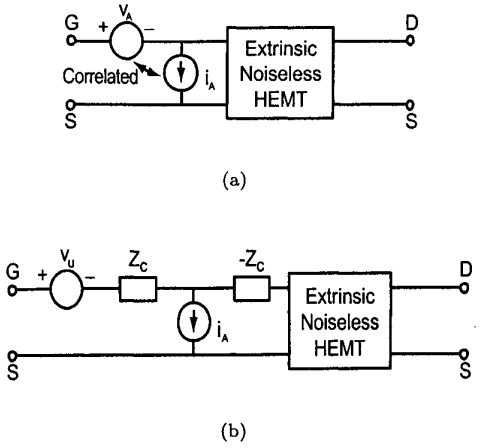

Fig. 1. (a) Equivalent noise circuit with noise sources (v_A and i_A) at the input (*ABCD* representation). (b) Equivalent noise circuit with two independent noise sources and correlation impedance ($v_A = Z_c i_A + v_u$).

We report here the extraction of the intrinsic noise sources and their correlation in AlGaN/GaN HEMTs. Using microwave noise and S-parameter measurements, the intrinsic noise sources were extracted by means of a modified deembedding routine suggested by Pucel *et al.* [9]. Then, the intrinsic noise sources and their values, deembedded at one frequency, were applied to the noise equivalent circuit model, and this model was used to simulate the noise parameters (i.e., NF_{min}, R_N, Y_{opt}) at other frequencies. This assumes that the microwave noise sources in the frequency range of interest are frequency independent (white noise) [10]. The agreement between the model simulation and the measured data is good.

II. Microwave Noise and S-parameter Measurement

The noise properties of AlGaN/GaN HEMTs, originally designed and fabricated for high power density op-

0-7803-7239-5/02/$10.00 © 2002 IEEE

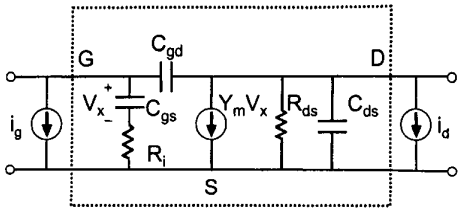

Fig. 2. Intrinsic noise equivalent circuit model (admittance form) with i_g and i_d representing partially correlated intrinsic noise sources. Inside the dashed box is now a noiseless two-port intrinsic transistor.

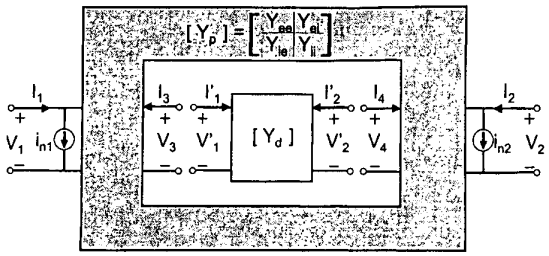

Fig. 3. Extrinsic transistor and its additional noise sources (i_{n1}, i_{n2}). The intrinsic transistor in Fig. 2 is embedded, represented by its admittance matrix, Y_d, and external parasitics are represented by the admittance matrix, Y_p (partitioned into four 2×2 submatrices, Y_{ee}, Y_{ei}, Y_{ie}, and Y_{ii}).

eration, were investigated. Details concerning the device fabrication and characteristics may be found elsewhere [11]. S-parameter data was obtained for 0.4×250 μm^2 AlGaN/GaN HEMTs on SiC substrates using a HP8510B vector network analyzer. On-wafer microwave noise measurements were performed using an ATN NP5B system. The frequency range (0.3-6 GHz) of the noise measurement was determined by the electric tuners used. The basic noise parameters, NF_{min}, R_N, and Y_{opt}, were extracted at various bias points from a load-pull measurement.

III. Theory

Figure 2 shows the noiseless intrinsic transistor small signal equivalent circuit with partially correlated noise sources, i_g and i_d. Circuit parameters inside the dashed box (as well as parasitics) are obtained from S-parameter measurements. The extrinsic transistor and its additional noise sources (i_{n1}, i_{n2}) are displayed in Fig. 3. Note that the intrinsic noise sources (i_g, i_d) in Fig. 2 are absorbed into i_{n1} and i_{n2} in Fig. 3 and that the parasitic admittance matrix, Y_p, is a 4×4 matrix to explain the four-port behavior. Using Y_d, Y_p (and its four 2×2 submatrices, Y_{ee}, Y_{ei}, Y_{ie}, and Y_{ii}), and the boundary condition ($V_3 = V_1'$, $V_4 = V_2'$, $I_3 = -I_1'$, $I_4 = -I_2'$) in Fig. 3, the extrinsic noiseless transistor and the noise sources (i_{n1}, i_{n2}) can be expressed as

$$\begin{bmatrix} I_1 \\ I_2 \end{bmatrix} = Y_e \begin{bmatrix} V_1 \\ V_2 \end{bmatrix} + \begin{bmatrix} i_{n1} \\ i_{n2} \end{bmatrix}, \quad (1)$$

where Y_e represents the two-port network for the extrinsic (intrinsic+parasitic) noiseless transistor, defined as

$$Y_e = Y_{ee} + WY_{ie}, \quad (2)$$

with

$$W = -Y_{ei}(Y_{ii} + Y_d)^{-1}. \quad (3)$$

A. Noise Correlation Matrix

Based on the theory of linear noisy two-ports [5], there are various methods to represent a noisy two-port. A model using the original network and the two additional noise sources (partially correlated) at its input (like in Fig. 1 (a)) is the *ABCD* (or chain) representation [12]. The equivalent noise circuit with two current noise sources, one at the input and the other at the output, is an example of the admittance representation (like in Fig. 2 and Fig. 3). Using the noise correlation matrix method [12], self- and cross- power spectral densities of the noise can be defined in each representation (e.g., *ABCD* or admittance), and transformation is possible from one to another. For example, the noise correlation matrix in Fig. 1 (a) can be defined as

$$C_A = \begin{bmatrix} v_A \\ i_A \end{bmatrix} \begin{bmatrix} v_A \\ i_A \end{bmatrix}^\dagger = \begin{bmatrix} < v_A v_A^* > & < v_A i_A^* > \\ < i_A v_A^* > & < i_A i_A^* > \end{bmatrix}, \quad (4)$$

where † denotes hermitian (complex conjugate transpose), <> the statistical average, and v_A and i_A are the two noise sources at the input of the noiseless two port system (*ABCD* form) in Fig. 1 (a). Similarly, C_d, the intrinsic noise correlation matrix (noise sources in Fig. 2), and C_{pd}, the extrinsic noise correlation matrix (noise sources in Fig. 3), are given in their admittance form by

$$C_d = \begin{bmatrix} i_g \\ i_d \end{bmatrix} \begin{bmatrix} i_g \\ i_d \end{bmatrix}^\dagger = \begin{bmatrix} < i_g i_g^* > & < i_g i_d^* > \\ < i_d i_g^* > & < i_d i_d^* > \end{bmatrix}, \quad (5)$$

$$C_{pd} = \begin{bmatrix} i_{n1} \\ i_{n2} \end{bmatrix} \begin{bmatrix} i_{n1} \\ i_{n2} \end{bmatrix}^\dagger = \begin{bmatrix} < i_{n1} i_{n1}^* > & < i_{n1} i_{n2}^* > \\ < i_{n2} i_{n1}^* > & < i_{n2} i_{n2}^* > \end{bmatrix}.$$

B. Noise Source Deembedding

The deembedding routine to extract the intrinsic noise sources (i_g, i_d) and their correlation for the AlGaN/GaN HEMT starts from C_A. The noise correlation matrix, C_A (in *ABCD* representation), can be obtained from the measured noise parameters. Then, C_A is transformed to its equivalent in admittance form, C_{pd}, so that after several matrix algebra steps (written in Matlab), the final intrinsic noise correlation matrix, C_d, is obtained. The detailed deembedding procedure is as follows.

First, the noise correlation matrix, C_A, as defined in (4), is obtained from the measured noise parameters (NF_{min}, R_N, and Y_{opt}) and expressed as [12]

$$C_A = \begin{bmatrix} R_N & \frac{NF_{min}-1}{2} - R_N Y_{opt}^* \\ \frac{NF_{min}-1}{2} - R_N Y_{opt} & R_N |Y_{opt}|^2 \end{bmatrix}. \quad (6)$$

Note that the noise correlation matrices throughout this work are normalized following the convention in [9]; all the

matrix elements are divided by $2kT_0B$, where k is Boltzmann's constant, T_0 is room temperature (290 Kelvin), and B is the noise bandwidth (1 Hz).

Second, the noise correlation matrix, C_A, obtained in (6), is transformed to the noise correlation matrix in admittance form, C_{pd}, by [9]

$$C_{pd} = VC_AV^\dagger, \tag{7}$$

where V is the transformation matrix (from $ABCD$ to admittance)

$$V = \begin{bmatrix} -Y_{e,11} & 1 \\ -Y_{e,21} & 0 \end{bmatrix}, \tag{8}$$

with $Y_{e,11}$ and $Y_{e,21}$ being elements of Y_e, the 2×2 matrix defined in (2).

Third, the noise contribution from the parasitic elements (i.e., C_p) should be stripped from the extrinsic transistor noise (C_{pd}) so that the final product of the deembedding routine, C_d, represents the normalized noise spectral power (self- and cross-correlated) of the intrinsic transistor only. The noise from the parasitic (passive) elements is thermal and uncorrelated with the intrinsic noise sources, i_g and i_d in Fig. 2. Generalizing Nyquist's theorem for linear networks, Twiss shows that $< i_m i_n^* > B = 2kT_0(y_{mn} + y_{nm}^*)B$, where $i_{m,n}$ is the short circuit noise current at the (m,n)th port and y_{mn} is an element of the network admittance matrix [13]. The noise correlation matrix of the parasitic network, C_p (in admittance form), can then be represented by

$$C_p = \frac{1}{2}(Y_p + Y_p^\dagger), \tag{9}$$

where Y_p is the admittance matrix of the 4-port parasitic network.

Finally, the correlation matrices (C_d, C_{pd}, C_p) are related by [9]

$$C_{pd} = C_{ee} + WC_{ie} + C_{ei}W^\dagger + W(C_{ii} + C_d)W^\dagger, \tag{10}$$

where C_{ee}, C_{ei}, C_{ie}, and C_{ii} are four submatrices partitioned from C_p with the same format as used for Y_p. By an inversion of the above matrix operation, the resulting noise correlation matrix for the intrinsic transistor, C_d, is obtained by

$$C_d = W^{-1}(C_{pd} - C_{ee})W^{-1\dagger} - C_{ie}W^{-1\dagger} - W^{-1}C_{ei} - C_{ii}. \tag{11}$$

From (5), the elements of C_d are represented by i_g (noise current at the input from gate to source), i_d (noise current at the output from drain to source), and their correlation. The correlation coefficient, C, is defined as

$$C = \frac{< i_d i_g^* >}{\sqrt{< |i_g|^2 >< |i_d|^2 >}}. \tag{12}$$

IV. Experimental Data

Figure 4 shows the intrinsic noise sources, i_g, i_d, and the correlation coefficient (magnitude), $|C|$, versus I_d. The intrinsic noise properties are obtained by the deembedding routine at each bias point (I_d is 10-90 mA with V_d set at 8 V,) for the 0.4×250 μm^2 AlGaN/GaN HEMT measured at 3 GHz. Note that i_d, increasing with the drain-to-source bias current, I_d, is the dominant noise source compared with i_g, and that i_g and $|C|$ are almost constant. Similar trends have been found in simulations [6], [7]. Figure 5 shows i_g, i_d, and $|C|$ versus frequency (1-5.5 GHz) on the same device measured at V_g = -4.2 V, V_d = 4 V (I_d = 20 mA, which is 80 mA/mm). As shown in Fig. 5, curves for

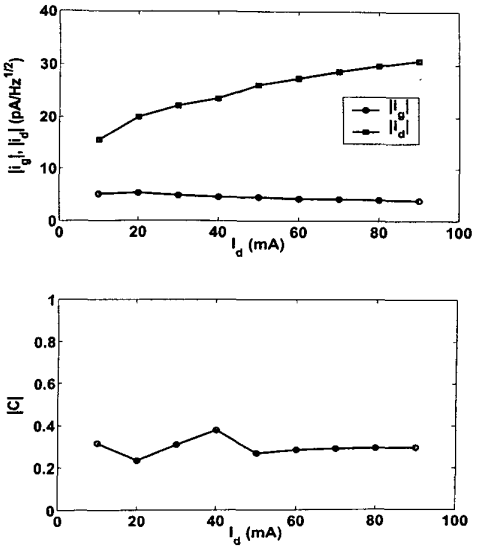

Fig. 4. Intrinsic noise sources, i_g, i_d in Fig. 2, and their correlation coefficient (magnitude), $|C|$, at 3 GHz. V_d = 8 V, and I_d is swept from 10 mA to 90 mA.

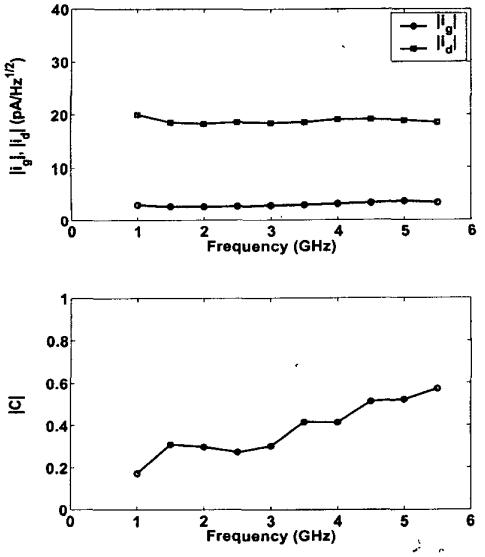

Fig. 5. Intrinsic noise sources, i_g, i_d in Fig. 2, and their correlation coefficient, $|C|$. Bias condition is V_g = -4.2 V, V_d = 4 V (I_d = 20 mA (80 mA/mm)).

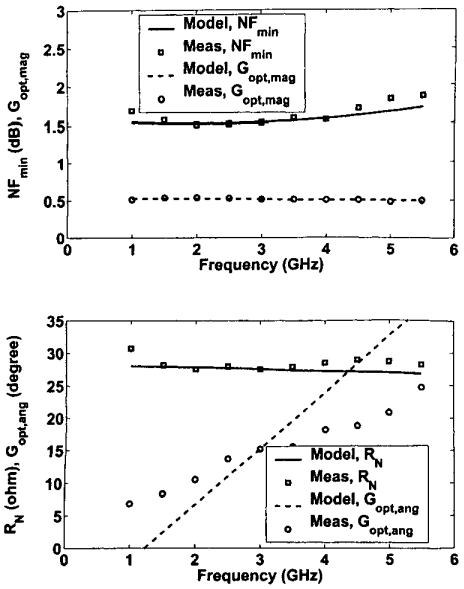

Fig. 6. Measured and modeled noise parameters at V_g = -4.2 V, V_d = 4 V (I_d = 20 mA), with frequency independent intrinsic noise sources. G_{opt} is the optimum noise reflection coefficient expressed as G_{opt} = (1-50Y_{opt})/(1+50Y_{opt}). The deembedding frequency is 3 GHz. The solid line (modeled) and square (measured) represent NF_{min} and R_N in each figure. The dashed line (modeled) and circle (measured) represent the magnitude and angle of G_{opt}.

the gate and drain noise sources are almost independent of frequency, although their correlation is found to be slightly increasing with frequency.

To validate the noise equivalent circuit model, the intrinsic noise correlation matrix, C_d, deembedded at one frequency (3 GHz), is used to simulate the noise parameters at other frequencies, assuming that the intrinsic noise sources and their correlation are frequency independent. Both the parasitic and intrinsic device equivalent circuits contain reactive components; thus, the admittance matrices Y_d and Y_p are frequency dependent and should be computed accordingly at other frequencies. Given C_d and C_p (from (9)), C_{pd} can be calculated using (10), and the new C_A (i.e., the new noise parameters) at other frequencies are obtained using the relation in (6). Figure 6 shows the simulated noise parameters from the model in comparison with the measured data at V_g = -4.2 V, V_d = 4 V (I_d = 20 mA). In Fig. 5, the extracted correlation between i_g and i_d is varying with frequency [14]. However, the simulated noise parameters using the intrinsic noise sources specified at one frequency (assumed to be frequency independent) show reasonably good agreement with the measured data.

V. Conclusion

The emphasis of this work is to determine the precise intrinsic noise sources for AlGaN/GaN HEMTs, thus enabling the development of an accurate noise equivalent circuit model. Using the measured noise parameters and the deembedding routine developed, gate and drain noise current sources and the correlation coefficient are extracted as a function of bias and frequency. The agreement between the measured and the modeled noise parameters is good. This work allows the study of noise mechanisms within the device and provides a tool for developing low noise device and circuit design concepts.

VI. Acknowledgment

The load-pull microwave noise measurement was performed at Motorola. The authors would like thank Dr. Chuck Weitzel, Digital DNA laboratories, Motorola, Tempe, AZ for his assistance and discussion on microwave noise measurements. This work was supported by ONR under contracts N00014-98-1-0371, N00014-99-C-0172, and N00014-98-1-0371 (John Zolper).

References

[1] V. Tilak, B. Green, V. Kaper, H. Kim, T. Prunty, J. Smart, J. Shealy, and L. Eastman, "Influence of barrier thickness on the high-power performance of AlGaN/GaN HEMT's," *IEEE Electron Device Lett.*, vol. 22, no. 11, pp. 504–506, Nov. 2001.

[2] S. L. Rumyantsev, N. Pala, M. S. Shur, E. Borovitskaya, A. P. Dmitriev, M. E. Levinshtein, R. Gaska, M. A. Khan, J. Yang, X. Hu, and G. Simin, "Generation-recombination noise in GaN/AlGaN heterostructure field effect transistors," *IEEE Trans. Electron Devices*, vol. 48, no. 3, pp. 530–534, Mar. 2001.

[3] W. Lu, J. Yang, M. A. Khan, and I. Adesida, "AlGaN/GaN HEMT's on SiC with over 100 GHz f_T and low microwave noise," *IEEE Trans. Electron Devices*, vol. 48, no. 3, pp. 581–585, Mar. 2001.

[4] T. Hussain, A. Kurdoghlian, P. Hashimoto, W. S. Wong, M. Wetzel, J. S. Moon, L. McCray, and M. Micovic, "GaN HFETs with excellent low noise performance at lower power levels through the use of thin AlGaN Schottky barrier layer," in *International Electron Devices Meeting Technical Digest*, 2001, pp. 581–584.

[5] H. Rothe and W. Dahlke, "Theory of noisy fourpoles," *Proc. IRE*, vol. 44, pp. 811–818, June 1956.

[6] H. Statz, H. A. Haus, and R. A. Pucel, "Noise characteristics of gallium arsenide field-effect transistors," *IEEE Trans. Electron Devices*, vol. 21, pp. 549–562, Sep. 1974.

[7] A. Cappy, "Noise modeling and measurement techniques," *IEEE Trans. Microwave Theory Tech.*, vol. 36, no. 1, pp. 1–10, Jan. 1988.

[8] M. W. Pospieszalski, "Modeling of noise paramters of MESFET's and MODFET's and their frequency and temperature dependence," *IEEE Trans. Microwave Theory Tech.*, vol. 36, no. 1, pp. 1–10, Jan. 1988.

[9] R. A. Pucel, W. Struble, R. Hallgren, and U. L. Rohde, "A general noise de-embedding procedure for packaged two-port linear active devices," *IEEE Trans. Microwave Theory Tech.*, vol. 40, no. 11, pp. 2013–2024, Nov. 1992.

[10] R. A. Pucel, H. A. Haus, and H. Statz, *Advances in Electronics and and Electron Physics*, vol. 38, New York: Academic Press., 1975.

[11] L. F. Eastman, V. Tilak, J. Smart B. M. Green, E. M. Chumbes, R. Dimitrov, H. Kim, O. S. Ambacher, N. Weimann, T. Prunty, M. Murphy, W. J. Schaff, and J. R. Shealy, "Undoped AlGaN/GaN HEMTs for microwave power amplification," *IEEE Trans. Electron Devices*, vol. 48, no. 3, pp. 479–485, Mar. 2001.

[12] H. Hillbrand and P. H. Russer, "An efficient method for computer aided noise analysis of linear amplifier networks," *IEEE Trans. on Circuit Syst.*, vol. 23, no. 4, pp. 235–238, Apr. 1976.

[13] R. Q. Twiss, "Nyquist's and Thevenin's theorems generalized for nonreciprocal linear networks," *J. Appl. Phys.*, vol. 26, no. 5, pp. 599–602, May 1955.

[14] W. Shockley, J. A. Copeland, and R. P. James, "The impedance field method of noise calculation in active semiconductor devices," in *Quantum Theory of Atoms, Molecules, and the Solid State*, 1966, pp. 537–563, New York: Academic Press.